

Syk promotes phagocytosis by inducing reactive oxygen species generation and suppressing SOCS1 in macrophage-mediated inflammatory responses

International Journal of
Immunopathology and Pharmacology
Volume 36: 1–13
© The Author(s) 2022
Article reuse guidelines:
sagepub.com/journals-permissions
DOI: 10.1177/03946320221133018
journals.sagepub.com/home/iji
SAGE

Young-Su Yi^{1,2,†}, Han Gyung Kim^{1,†}, Ji Hye Kim^{1,†}, Woo Seok Yang¹, Eunji Kim¹, Jae Gwang Park¹, Nur Aziz¹, Narayanan Parameswaran³ and Jae Youl Cho¹ 

Abstract

Objective: Inflammation, a vital innate immune response against infection and injury, is mediated by macrophages. Spleen tyrosine kinase (Syk) regulates inflammatory responses in macrophages; however, its role and underlying mechanisms are uncertain.

Materials and Methods: In this study, overexpression and knockout (KO) cell preparations, phagocytosis analysis, confocal microscopy, reactive oxygen species (ROS) determination, mRNA analysis, and immunoprecipitation/western blotting analyses were used to investigate the role of Syk in phagocytosis and its underlying mechanisms in macrophages during inflammatory responses.

Results: Syk inhibition by Syk KO, Syk-specific small interfering RNA (siSyk), and a selective Syk inhibitor (piceatannol) significantly reduced the phagocytic activity of RAW264.7 cells. Syk inhibition also decreased cytochrome c generation by inhibiting ROS-generating enzymes in lipopolysaccharide (LPS)-stimulated RAW264.7 cells, and ROS scavenging suppressed the phagocytic activity of RAW264.7 cells. LPS induced the tyrosine nitration (N-Tyr) of suppressor of cytokine signaling 1 (SOCS1) through Syk-induced ROS generation in RAW264.7 cells. On the other hand, ROS scavenging suppressed the N-Tyr of SOCS1 and phagocytosis. Moreover, SOCS1 overexpression decreased phagocytic activity, and SOCS1 inhibition increased the phagocytic activity of RAW264.7 cells.

Conclusion: These results suggest that Syk plays a critical role in the phagocytic activity of macrophages by inducing ROS generation and suppressing SOCS1 through SOCS1 nitration during inflammatory responses.

Keywords

Syk, phagocytosis, reactive oxygen species, SOCS1, nitration, inflammation

¹Department of Integrative Biotechnology, Sungkyunkwan University, Suwon, Korea

²Department of Life Sciences, Kyonggi University, Suwon, Korea

³Department of Physiology and Division of Pathology, Michigan State University, East Lansing, MI, USA

[†]These authors contributed equally to this work.

Corresponding authors:

Young-Su Yi, Department of Life Sciences, Kyonggi University, 154-42 Gwanggyosan-ro, Yeongtong-gu, Suwon, Gyeonggi-do 16227, Korea.
Email: ysyi@kgu.ac.kr

Jae Youl Cho, Department of Integrative Biotechnology, Sungkyunkwan University, 2066 Seobu-ro, Jangan-gu, Suwon Gyeonggi-do 16419, Korea.
Email: jaecho@skku.edu



Creative Commons Non Commercial CC BY-NC: This article is distributed under the terms of the Creative Commons Attribution-NonCommercial 4.0 License (<https://creativecommons.org/licenses/by-nc/4.0/>) which permits non-commercial use, reproduction and distribution of the work without further permission provided the original work is attributed as specified on the SAGE and Open Access pages (<https://us.sagepub.com/en-us/nam/open-access-at-sage>).

Background

Inflammation is an innate immune response mediated mainly by myeloid immune cells such as macrophages to protect the body from infection by various pathogens and respond to cellular danger signals.^{1,2} The inflammatory response occurs as a result of interactions between pattern recognition receptors and pathogen-associated molecular patterns (PAMPs) and danger-associated molecular patterns.¹⁻³ Those interactions activate inflammatory signaling pathways, such as the nuclear factor-kappa B (NF- κ B), activator protein-1 (AP-1), and interferon regulatory factor (IRF) pathways.⁴⁻⁷ Activation of these inflammatory signaling pathways is mediated by initiation of signal transduction cascades that activate a variety of intracellular signaling molecules, such as spleen tyrosine kinase (Syk), phosphoinositide 3-kinase, Akt, inhibitor of κ B (I κ B) kinase α/β (IKK α/β), and I κ B in the NF- κ B signaling pathway; c-Jun N-terminal kinase, p38, and extracellular signal-regulated kinase in the AP-1 signaling pathways; and TANK, TANK-binding kinase 1, and IKK ϵ in the IRF signaling pathway.⁴⁻⁷ As a result of activation of these inflammatory signaling pathways, macrophages induce inflammatory responses in various ways, such as by facilitating the generation of reactive oxygen species (ROS) and reactive nitrogen species, phagocytosis, and the expression of pro-inflammatory cytokines and inflammatory enzymes.⁴⁻⁹ Although inflammation is a protective immune response, chronic inflammation rearranges tissue architecture and destroys tissues and is involved in the pathogenesis of many inflammatory and autoimmune diseases and even cancers.¹⁰⁻¹⁶ Therefore, many efforts have been made to discover the molecular mechanisms that induce inflammatory responses, identify and validate molecular targets to suppress inflammatory responses, and develop therapeutic agents to ameliorate the symptoms of those diseases.

Syk is a non-receptor tyrosine kinase that belongs to the tyrosine kinase family. Syk has three main domains: an N-terminal Src homology 2 domain, a C-terminal Src homology 2 domain, and a kinase domain.⁶ An alternatively spliced form of Syk, Syk-B, has been identified in some cells,¹⁸ but the exact function of Syk-B and its alternative splicing mechanisms are unknown. The structure of Syk is highly conserved among species. Human and murine Syk share 92% of their amino acids, and Syk-like molecules are found in other species, including rats, pigs, fruit flies, and hydras.¹⁷⁻²⁰ Syk is widely expressed in hematopoietic and non-hematopoietic cells, such as immune cells, neuronal cells, epithelial cells, vascular endothelial cells, and fibroblasts,⁶ and it catalyzes the phosphorylation of numerous proteins at their tyrosine residues,²¹ which serve as scaffolds to downstream effector proteins for subsequent activation, including signaling molecules activated in the

NF- κ B signaling pathway.^{6,22,23} Syk is a critical player in a diverse variety of biological functions, including inflammatory responses, cellular adhesion, innate pathogen recognition, tissue damage recognition, antibody-dependent cellular cytotoxicity, bone metabolism, platelet functioning, and vascular development.^{6,23}

Although Syk has been demonstrated to play critical roles in inflammatory responses and diseases,^{6,24-27} its nuanced function in the inflammatory response and the molecular mechanisms underlying that function remain unknown. Therefore, this study investigated the regulatory role of Syk in the phagocytic activity of macrophages by regulating ROS generation and posttranslational modification of SOCS1 during inflammatory responses.

Methods

Materials

Roswell Park Memorial Institute 1640 (RPMI 1640) cell culture medium, Dulbecco's Modified Eagle's medium (DMEM), fetal bovine serum (FBS), streptomycin, penicillin, L-glutamine, phosphate-buffered saline (PBS), Lipofectamine[®] 2000, mounting medium, TRIZOL[™] reagent, MuLV reverse transcriptase, *pfu* DNA polymerase, DH5 α competent cells, polyvinylidene difluoride (PVDF) membranes, enhanced chemiluminescence (ECL) reagent, and Texas Red-X phalloidin were purchased from Thermo Fisher Scientific (Waltham, MA, USA). LentiCRISPRv2 vector was purchased from Addgene (Watertown, MA, USA). Puromycin dihydrochloride, lipopolysaccharide (LPS, *Escherichia coli* 0111:B4), dihydrorhodamine 123 (DHR 123), fluorescein isothiocyanate-*Escherichia coli* (FITC-*E.coli*), piceatannol (Pic), bovine serum albumin (BSA), α -tocopherol, resveratrol, N(G)-nitro-L-arginine methyl ester (L-NAME), sodium nitroprusside (SNP), and sodium dodecyl sulfate (SDS) were purchased from Sigma-Aldrich (St. Louis, MO, USA). Antibodies specific for LAMP-1 (ab25245), FITC (sc-69872), N-Tyr (ab24497), SOCS1 (ab9870), Syk (CST 2712), Flag (CST 8146), and β -actin (CST 4967), which were used for western blot analysis, immunoprecipitation, and immunofluorescence staining, were purchased from Abcam (Cambridge, UK), Cell Signaling Technology (Beverly, MA, USA), Santa Cruz Biotechnology, Inc. (Dallas, TX, USA), Upstate Biotechnology (Waltham, MA, USA), and NewEast Biosciences (Malvern, PA, USA). A QIAprep Spin Miniprep Kit was purchased from Qiagen, Inc. (Germantown, MD, USA). Small interfering RNA (siRNA) specific for Syk (siSyk) and SOCS1 (siSOCS1) was purchased from Genolution (Seoul, Korea). The primers used for quantitative real-time polymerase chain reaction (PCR) were synthesized at Macrogen Inc. (Seoul, Korea). SYBR Premix Ex Taq was sourced from Takara

Bio Inc. (Shiga, Japan). Protein A-coupled Sepharose® beads were supplied by GE Healthcare Life Sciences (Marlborough, MA, USA).

Cell culture and transfection

RAW264.7 cells and human embryonic kidney 293 (HEK293) cells were purchased from the American Type Culture Collection (Rockville, MD, USA). The cells were cultured in RPMI 1640 medium and DMEM, respectively, supplemented with 10% heat-inactivated FBS, streptomycin (100 mg/ml), penicillin (100 U/ml), and L-glutamine (2 mM) at 37°C in a humidified incubator with 5% CO₂. Mycoplasma contamination was tested using a BioMycoX Mycoplasma PCR Detection Kit (CellSafe, Seoul, Korea). RAW264.7 and HEK293 cells were transfected with either expression constructs or siRNA (Table 1) or sgRNA (Table 2) constructs for 48 h using Lipofectamine® 2000 according to the manufacturer's instructions.

Generation of Syk^{-/-} RAW264.7 cells by the CRISPR/Cas9 system

Small guide RNA (sgRNA) sense and antisense oligos specific for Syk were synthesized, and the sgRNA hybrid was inserted into a lentiCRISPRv2 vector as previously described.^{28,29} RAW264.7 cells were transfected with the Syk sgRNA construct using Lipofectamine® 2000 according to the manufacturer's instructions, and the transfected RAW264.7 cells were selected using puromycin (1.0 mg/ml) in RPMI 1640 medium containing 10% heat-inactivated FBS until all non-transfected RAW264.7 cells were dead.

Phagocytosis assay

RAW264.7 cells were incubated with FITC-*E.coli* (10 µg/ml) for the indicated times. After being washed with PBS,

Table 1. The siRNA sequences used in this study.

Target		Sequence (5' to 3')
Syk	Sense	CGAUUUCGGUCUUUCCAAAUU
	Anti-sense	UUUGGAAAGACCGAAAUUCGUU
SOCS1	Sense	GUGACUACCUGAGUUCUUUUU
	Anti-sense	AAGGAACUCAGGUAGUCACUU

Table 2. The sgRNA sequences used in this study.

Target		Sequence (5' to 3')
Syk	Sense	TCGCAATTACTIONACTACGACG
	Anti-sense	CGTCGTAGTAGTAATTGCGA

the cells were resuspended in FACS buffer, and the fluorescence of the cells was quantified using a fluorescence microplate reader and a flow cytometer.

Confocal microscopy

RAW264.7 cells were transfected with either control scrambled siRNA (siN.C) or siSyk for 24 h. The RAW264.7 cells were treated with vehicle (DMSO), α-tocopherol (100 µM), or resveratrol (50 µM) for 12 h and incubated with FITC-*E.coli* (10 µg/ml) for the indicated times. The cells were fixed with formaldehyde (4%) for 10 min, washed with PBS three times for 5 min each, and permeabilized with Triton X-100 (1%) for 5 min at room temperature. After being washed with PBS three times for 5 min each, the cells were incubated with BSA for blocking and then incubated with primary antibodies specific for LAMP-1 or FITC, followed by secondary antibody incubation at 4°C for 1 h. After being washed with PBS three times for 5 min each, the cells were covered with a cover glass in mounting medium (20 µl) and analyzed by confocal microscopy.

ROS generation assay

RAW264.7 cells treated with LPS (1 µg/ml) at 37°C for the indicated times were incubated with DHR 123 (20 µM) at 37°C for 20 min. After being washed three times with PBS, the cells were resuspended in FACS buffer (2% BSA and 0.1% sodium azide in PBS), and the fluorescence of the cells was determined using a flow cytometer.

Western blot analysis

RAW264.7 cells were lysed in ice-cold buffer A (pH 7.4, 20 mM Tris-HCl, 2 mM EDTA, 2 mM EGTA, 50 mM glycerol phosphate, 1 mM DTT, 2 µg/ml aprotinin, 2 µg/ml leupeptin, 1 µg/ml pepstatin, 50 µM PMSF, 1 mM benzamide, 2% Triton X-100, 10% glycerol, 0.1 mM sodium vanadate, 1.6 mM pervanadate, and 20 mM NaF) on ice for 30 min, followed by centrifugation at 12,000 rpm for 5 min at 4°C. The supernatant was collected as a whole-cell lysate and stored at -20°C until use. The whole-cell lysates were subjected to SDS polyacrylamide gel electrophoresis and transferred to PVDF membranes. The membranes were blocked with blocking buffer (5% BSA in Tris-buffered saline) at room temperature for 1 h and then incubated with primary antibodies specific for each target at room temperature for 1 h. After being washed with washing buffer (pH 7.6, Tris-base, NaCl, and 0.1 % Tween 20) three times for 10 min each, the membranes were incubated with HRP-linked secondary antibodies at room temperature for 1 h. After being washed three times, the target proteins were visualized with ECL reagent.

Quantitative real-time polymerase chain reaction

Total RNA was extracted using TRIZOL™ reagent according to the manufacturer's instructions and immediately stored at -70°C until use. Then, 1 μg of the total RNA was used to synthesize cDNA using MuLV reverse transcriptase, and the cDNA was used for quantitative real-time PCR with SYBR Premix Ex Taq according to the manufacturer's instructions. The primer sequences used for quantitative real-time PCR are listed in Table 3.

Immunoprecipitation

The whole-cell lysates (500 μg exogenous and 1 mg endogenous protein) were pre-cleared using 10 μl of protein A-coupled Sepharose® beads (50% v/v) at 4°C for 1 h, and the pre-cleared whole-cell lysates were incubated with primary antibodies specific for each target at 4°C overnight with gentle rotation. The immunocomplexes were again incubated with protein A-coupled Sepharose® beads (50% v/v) at 4°C for 4 h with gentle rotation, and the supernatant was removed from the beads by centrifugation. After the beads were washed with ice-cold buffer A five times, they were resuspended in protein sample buffer (pH 6.8, 50 mM Tris-HCl, 2% SDS, 10% glycerol, 1% β -mercaptoethanol, 12.5 mM EDTA, and 0.02% bromophenol blue) and boiled for 10 min. Then the immunoprecipitates were subjected to western blot analysis to detect target proteins.

Statistical analysis

The data presented in this study are expressed as the mean \pm standard deviation of at least three independent experiments. For statistical comparison, all results were analyzed by either analysis of variance or the Mann-Whitney U test, and p values less than 0.05 were considered statistically significant ($*p < 0.05$, $**p < 0.01$). All statistical analyses were conducted using the SPSS program (ver. 27.0, SPSS Inc., Chicago, IL, USA).

Results

Syk was essential for phagocytic activity in macrophages

Macrophages are effector cells that phagocytose pathogens to induce innate immune responses,³⁰ and the role of Syk in phagocytosis of macrophages was investigated. To examine the effect of Syk on phagocytosis in macrophages, Syk knock-out (Syk^{-/-}) RAW264.7 cells were generated (Figure 1(a)), and their phagocytic activity was examined. Phagocytic activity was increased in the wild-type (WT)

Table 3. Primer sequences used for quantitative real-time PCR in this study.

Target	Primer	Sequence (5' to 3')
iNOS	Forward	GGAGCCTTTAGACCTCAACAGA
	Reverse	TGAACGAGGAGGGTGGTG
NOX1	Forward	ATCTTCGCGAAACCCGTGAT
	Reverse	AGAATCACAGCGAGATGGCTT
AOC3	Forward	CAGCTCGGGACAGTGAGATA
	Reverse	CCAGGTCTCAGCAAAGACAA
AOXI	Forward	CAACCTTCCATCCAACACTG
	Reverse	CCACATTTGATTGCCACTC
XDH	Forward	GCGATTGCTACACTCCAGA
	Reverse	AGGGTTGAGGTCAGAGATGG
GAPDH	Forward	CAATGAATACGGCTACAGCAAC
	Reverse	AGGGAGATGCTCAGTGTGG

RAW264.7 cells at 10, 20, and 30 min, whereas it was markedly suppressed in the Syk^{-/-} RAW264.7 cells (Figures 1(a) and (b)). The role of Syk in phagocytosis was also investigated in Syk-deficient RAW264.7 cells. Phagocytic activity was markedly suppressed at 10, 20, and 30 min in RAW264.7 cells transfected with siSyk (20 nM) (Figures 1(c) and (d)) and in those treated with Pic (50 μM) (Figures 1(e) and (f)). Whether Syk-induced phagocytosis in macrophages was lysosome-dependent was examined next. Confocal microscopic analysis confirmed phagocytic activity to be decreased in the siSyk-transfected RAW264.7 cells compared with WT RAW264.7 cells at 60 and 120 min, and Syk-induced phagocytosis occurred in a lysosome-dependent manner (Figure 1(g)). These results clearly indicate that Syk is a key player in the phagocytic activity of macrophages.

ROS were a critical determinant of Syk-induced phagocytosis in macrophages

The role of ROS generation in Syk-induced phagocytosis was investigated in macrophages. Because LPS induces ROS generation in macrophages,³¹ RAW264.7 cells were treated with LPS, and ROS generation was examined in WT and Syk-deficient RAW264.7 cells. ROS generation increased time-dependently for 25–35 min following LPS treatment and decreased after 35 min (Figure 2(a)). The effect of Syk on ROS generation was examined for up to 30 min in RAW264.7 cells. LPS-induced ROS generation was significantly inhibited in Syk^{-/-} RAW264.7 cells at 10, 20, and 30 min after treatment compared with that in WT RAW264.7 cells (Figure 2(b)). LPS-induced ROS generation was also significantly inhibited in siSyk-transfected RAW264.7 cells (Figure 2(c)) and RAW264.7 cells treated with Pic, a selective Syk inhibitor,^{32,33} at 10, 20, and 30 min compared with that in

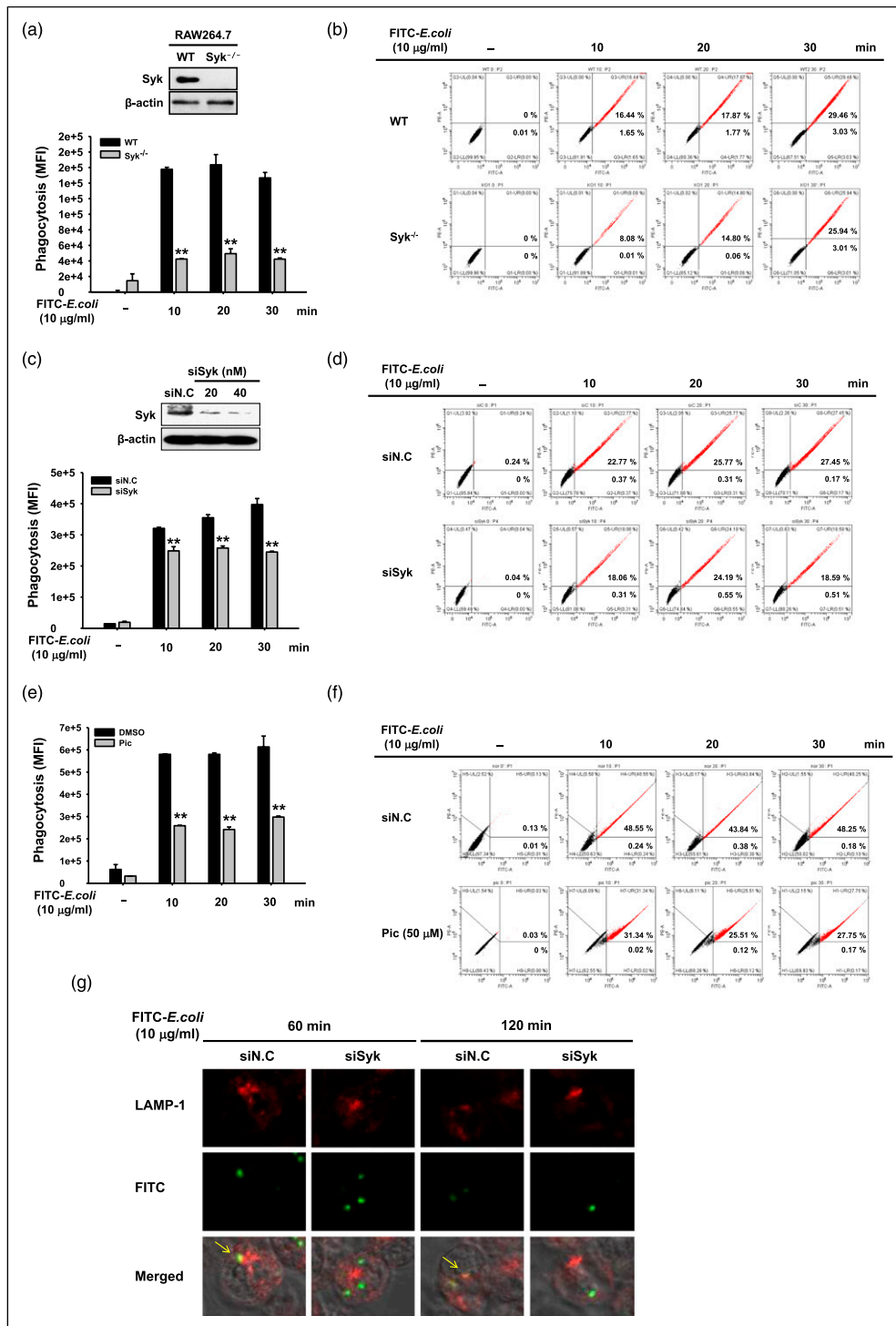


Figure 1. Syk was essential for phagocytic activity in macrophages. (a) Syk expression in WT and *Syk*^{-/-} RAW264.7 cells. WT and *Syk*^{-/-} RAW264.7 cells were incubated with FITC-*E.coli* (10 μ g/ml) for the indicated times, and fluorescence was quantified by (a) a fluorescence plate reader and (b) a flow cytometer. RAW264.7 cells transfected with siN.C.- or siSyk (20 nM) for 24 h were incubated with FITC-*E.coli* (10 μ g/ml) for the indicated times, and fluorescence was determined using (c) a fluorescence plate reader and (d) a flow cytometer. RAW264.7 cells treated with vehicle (DMSO) or Pic (50 μ M) were incubated with FITC-*E.coli* (10 μ g/ml) for the indicated times, and fluorescence was determined using (e) a fluorescence plate reader and (f) a flow cytometer. (g) RAW264.7 cells transfected with siN.C.- or siSyk were incubated with FITC-*E.coli* (10 μ g/ml) for the indicated times, and the fluorescence of LAMP-I and FITC was visualized using confocal microscopy. The arrow indicates the overlap of LAMP-I and FITC fluorescence. N.C., negative control. ***p* < 0.01 compared with controls.

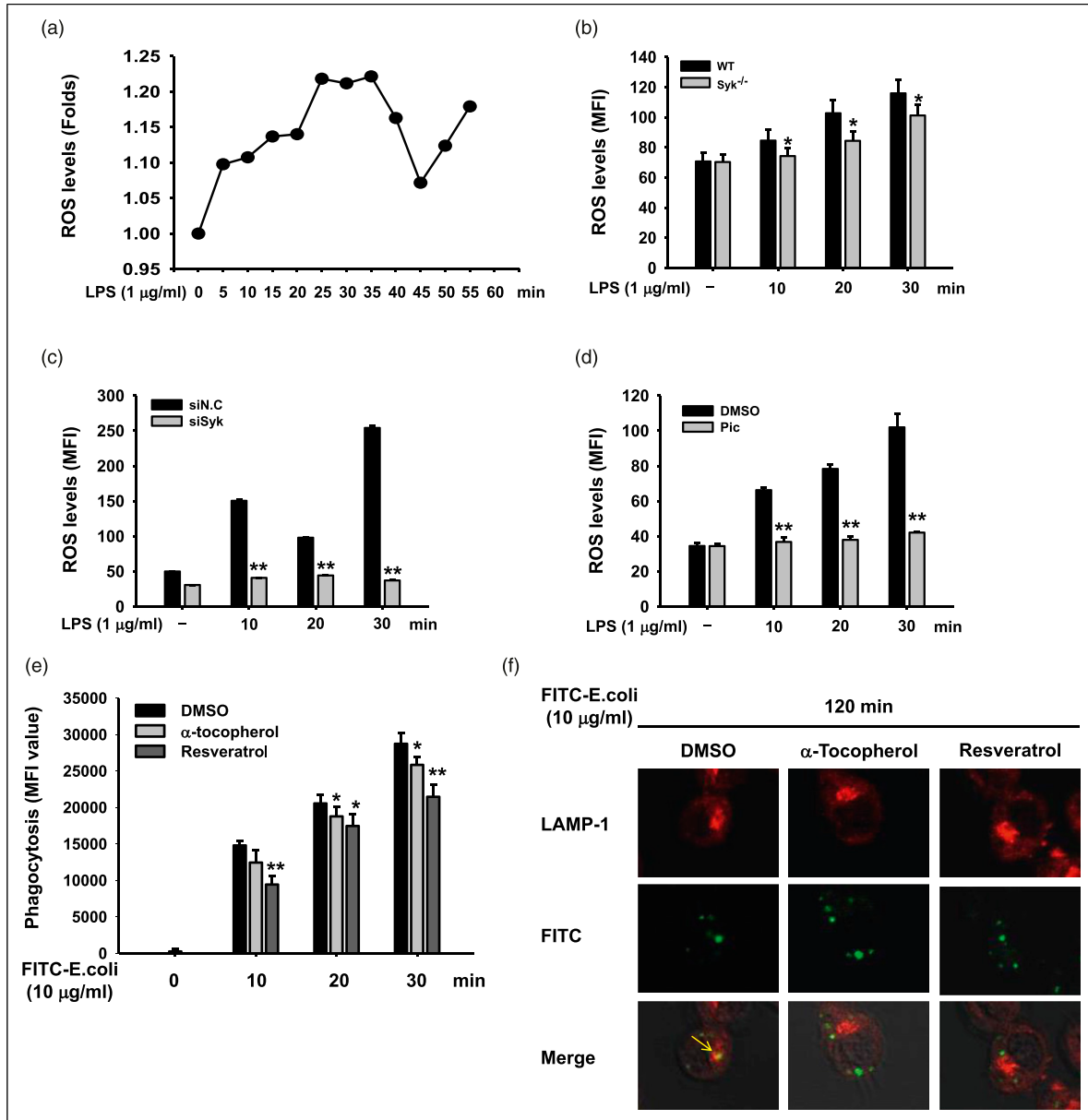


Figure 2. ROS was a critical determinant of Syk-induced phagocytosis in macrophages. (a) RAW264.7 cells treated with LPS (1 µg/ml) for the indicated times were incubated with DHR 123 (20 µM) for 20 min, and the ROS level was determined by fluorescence quantification. (b) WT and Syk^{-/-} RAW264.7 cells, (c) siN.C. or siSyk-transfected RAW264.7 cells, and (d) DMSO- (vehicle) and Pic-treated (50 µM) RAW264.7 cells were treated with LPS (1 µg/ml) for the indicated times and incubated with DHR 123 (20 µM) for 20 min. The ROS level was determined by measuring fluorescence using a fluorescence plate reader. (e) RAW264.7 cells treated with DMSO (vehicle), α-tocopherol (100 µM), or resveratrol (50 µM) for 12 h were incubated with FITC-*E.coli* (10 µg/ml) for the indicated times, and fluorescence was determined using a fluorescence plate reader. (f) RAW264.7 cells treated with vehicle (DMSO), α-tocopherol (100 µM), or resveratrol (50 µM) for 12 h were incubated with FITC-*E.coli* (10 µg/ml) for 120 min, and the fluorescence of LAMP-I and FITC was visualized using confocal microscopy. The arrow indicates the overlap of LAMP-I and FITC fluorescence. N.C., negative control. *p < 0.05, **p < 0.01 compared with controls.

WT RAW264.7 cells (Figure 2(d)). Next, the effect of ROS on phagocytosis in macrophages was examined. RAW264.7 cells were treated with either α-tocopherol or resveratrol, both of which inhibit ROS generation,^{34–37} and phagocytic activity was determined in those cells.

Phagocytic activity was significantly inhibited by both α-tocopherol and resveratrol in RAW264.7 cells at 10–30 min post-treatment (Figure 2(e)). Confocal microscopic analysis confirmed that the reduction of ROS generation by both α-tocopherol and resveratrol inhibited

lysosome-dependent phagocytosis in RAW264.7 cells at 120 min (Figure 2(f)). These results suggest that Syk rapidly (within 30 min) induces ROS generation, which, in turn, induces phagocytosis in macrophages. Thus, Syk induces phagocytosis by promoting ROS generation in macrophages.

Syk upregulated the expression of ROS-generating enzymes

Because Syk induced phagocytic activity by increasing ROS generation in macrophages, the molecular mechanism of Syk-induced ROS generation was investigated. Enzymes critical for ROS generation have been identified, and the effect of Syk on the gene expression of those ROS-

generating enzymes was examined in RAW264.7 cells. Because ROS generation increased gradually for 25 to 30 min after LPS treatment (Figure 2(a)), the mRNA expression of ROS-generating enzymes was examined in RAW264.7 cells treated with LPS for up to 30 min. The mRNA expression of the ROS-generating enzymes iNOS, NADPH oxidase 1 (NOX1), aldehyde oxidase 1 (AOX1), and xanthine dehydrogenase (XDH) increased following LPS treatment, with the highest level at 10 min, whereas the mRNA expression of amine oxidase copper containing-3 (AOC3) increased gradually for up to 30 min following LPS treatment in RAW264.7 cells (Figure 3(a)). The LPS-induced mRNA expression of iNOS, NOX1, AOX1, and XDH was significantly inhibited in Syk^{-/-} RAW264.7 cells compared with WT RAW264.7 cells (Figure 3(b)).

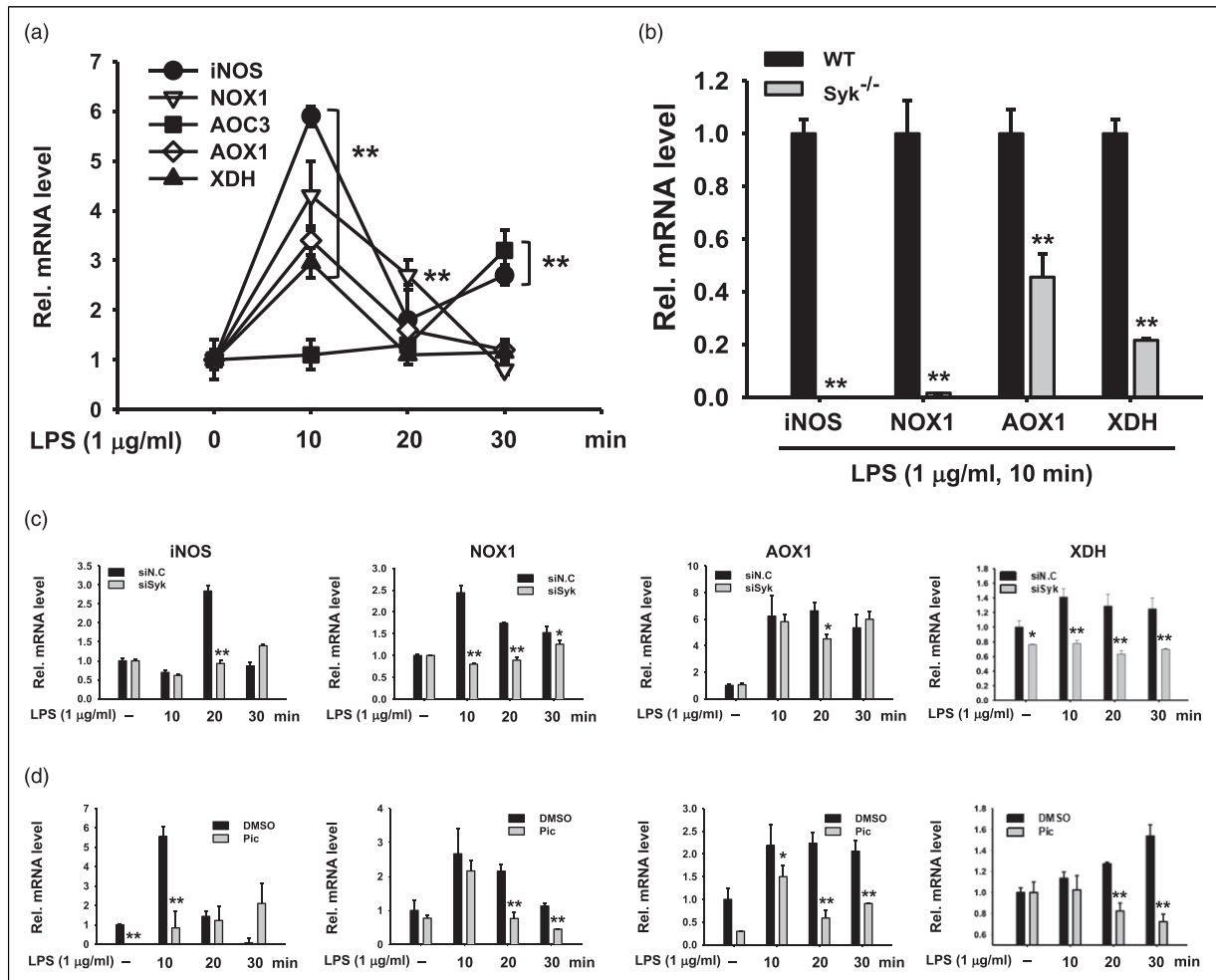


Figure 3. Syk upregulated the expression of ROS-generating enzymes. (a) RAW264.7 cells were treated with LPS (1 µg/ml) for the indicated times, and the mRNA expression of iNOS, NOX1, AOC3, AOX1, and XDH was determined using quantitative real-time PCR. (b) WT and Syk^{-/-} RAW264.7 cells were treated with LPS (1 µg/ml) for 10 min, and mRNA expression of iNOS, NOX1, AOX1, and XDH was determined by quantitative real-time PCR. (c) siN.C- or siSyk-transfected RAW264.7 cells and (d) DMSO- (vehicle) and Pic-treated (50 µM) RAW264.7 cells were treated with LPS (1 µg/ml) for the indicated times, and mRNA expression of iNOS, NOX1, AOX1, and XDH was determined using quantitative real-time PCR. **p* < 0.05, ***p* < 0.01 compared with controls.

The LPS-induced mRNA expression of those enzymes was also inhibited in the siSyk-transfected RAW264.7 cells (Figure 3(c)) and the RAW264.7 cells treated with Pic (50 μ M) (Figure 3(d)). These results suggest that Syk induces ROS generation in macrophages by upregulating the expression of ROS-generating enzymes, which further suggests that Syk-induced ROS generation and phagocytosis are mediated by an increase in the expression of ROS-generating enzymes in macrophages.

SOCS1 negatively regulated phagocytic activity in macrophages via nitration

We investigated how the ROS produced by ROS-generating enzymes regulated phagocytosis in macrophages. Interestingly, protein nitration profile screening identified tyrosine-nitrated (N-Tyr) proteins with molecular weights around 98, 39, and 23 kDa in LPS-stimulated RAW264.7 cells, and the N-Tyr levels in those cells increased gradually, with the highest levels occurring 30–40 min after stimulation (Figure 4(a)). Immunoprecipitation and western blot analyses identified the 23-kDa N-Tyr protein in the LPS-stimulated RAW264.7 cells as SOCS1 (Figure 4(b)); however, the other two N-Tyr proteins were not identified by immunoprecipitation or western blot analysis (data not shown). This result was confirmed by the increased N-Tyr of SOCS1 produced by SNP, an ROS-generating agent,³⁸ in SOCS1-transfected HEK293 cells (Figure 4(c)). As expected, the N-Tyr of SOCS1 induced by LPS was inhibited dramatically by the iNOS inhibitor L-NAME and radical scavengers such as α -tocopherol (Figure 4(d)).^{34,35,39} These results suggest that the N-Tyr of SOCS1 is induced by ROS generation in macrophages. Because Syk induced phagocytic activity by increasing ROS generation in RAW264.7 cells (Figure 2), the role of SOCS1 in the phagocytic activity of macrophages was examined. Phagocytic activity was significantly reduced in SOCS1-overexpressing RAW264.7 cells (Figure 4(e)), and inhibition of SOCS1 expression by siSOCS1 induced phagocytic activity in RAW264.7 cells (Figure 4(f)), indicating that SOCS1 acts as a negative regulator of macrophage-mediated phagocytosis. The effect of ROS in SOCS1-inhibited phagocytic activity in macrophages was examined next. SNP treatment increased the phagocytic activity inhibited by SOCS1 to that of WT RAW264.7 cells (Figure 4(g)). Collectively, these results indicate that ROS generated in macrophages by LPS or SNP stimulation induced SOCS1 inhibition by nitration at its tyrosine residues, leading to phagocytosis. Therefore, Syk induces phagocytosis in macrophages by inhibiting SOCS1 activity through the nitration of SOCS1.

Discussion

ROS generation and phagocytosis are critical processes in the inflammatory response in macrophages; however, little is known about the molecular mechanism by which ROS generation occurs or its effect on phagocytosis in the macrophage-mediated inflammatory response. Previous studies have demonstrated that stimulating macrophages with PAMPs such as LPS induces ROS generation and phagocytosis,⁴⁰ and that many intracellular signaling molecules, such as Syk, are activated in macrophages during the inflammatory response.^{4,6,7,41} Despite those previous studies, the role of Syk in phagocytosis, a key innate immune response in macrophages, is poorly understood, and the corresponding molecular mechanism was unidentified. This study demonstrates that Syk is an essential player in phagocytosis in macrophages, inducing ROS generation by upregulating the expression of ROS-generating enzymes and inhibiting SOCS1 activity through a posttranslational modification of SOCS1. In this study, Syk-deficient conditions were generated in macrophages (RAW264.7 cells) in three ways: Syk KO by the CRISPR/Cas9 system and Syk inhibition by siSyk or Pic, a selective Syk inhibitor. Regardless of the method, Syk inhibition significantly inhibited phagocytic activity in Syk-deficient RAW264.7 cells from 10 to 30 min following LPS treatment (Figure 1). Phagosomes are fused with lysosomes in macrophages, leading to proteolysis of phagocytosed bacteria.^{42,43} Consistent with that observation, Syk-induced phagocytosis involved fusion with lysosomes in RAW264.7 cells, but that fusion between phagosomes and lysosomes was suppressed in Syk-deficient RAW264.7 cells (Figure 1(g)). These results strongly suggest that Syk is an essential player that rapidly promotes phagocytosis, and that lysosomal fusion and degradation are required for Syk-induced phagocytosis in macrophages.

ROS have a variety of biological functions, including induction of signal transduction required for macrophage differentiation and activation and killing of pathogens through respiratory bursts.⁴⁴ This study confirmed that ROS generation is correlated with phagocytosis in macrophages. ROS generation was induced beginning 5 min after LPS stimulation and was highest at around 30 min (Figure 2(a)). The rapid LPS-stimulated generation of ROS was induced by Syk, and ROS generation was decreased in Syk-deficient RAW264.7 cells, indicating that Syk is a critical factor for ROS generation in macrophages. These results suggest that ROS generated by Syk could induce phagocytosis in macrophages, and ROS scavenging by α -tocopherol and resveratrol suppressed phagocytosis in macrophages (Figures 2(e) and (f)). Thus, Syk promotes phagocytosis by inducing ROS generation in macrophages during the inflammatory response.

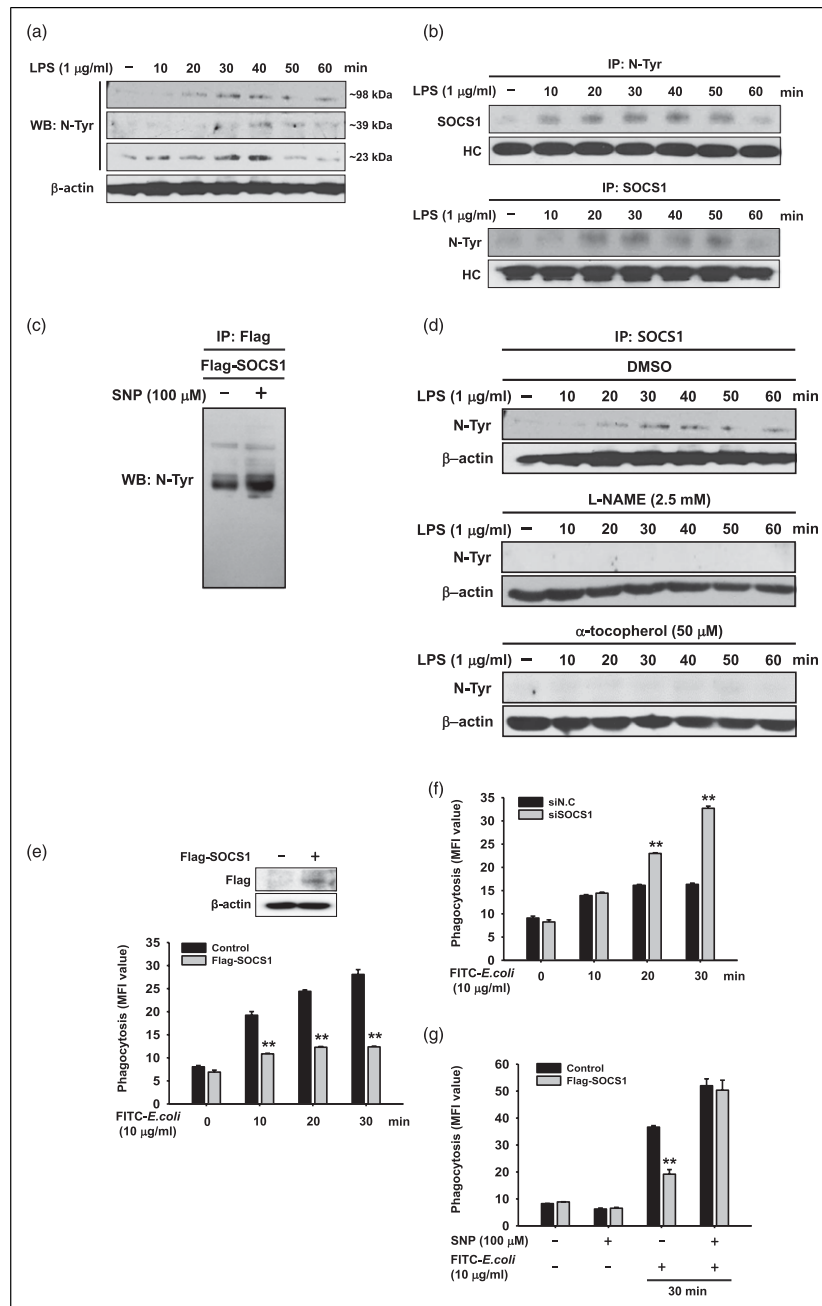


Figure 4. SOCS1 negatively regulated phagocytic activity via nitration in macrophages. (a) N-Tyr proteins in the whole-cell lysates of RAW264.7 cells treated with LPS (1 μ g/ml) for the indicated times were detected by western blot analysis. (b) N-Tyr SOCS1 in the whole-cell lysates of RAW264.7 cells treated with LPS (1 μ g/ml) for the indicated times was detected by immunoprecipitation and western blot analysis. (c) HEK293 cells transfected with a Flag-SOCS1 plasmid for 48 h were treated with either vehicle (DMSO) or SNP (100 μ M) for 3 h, and N-Tyr SOCS1 was detected by immunoprecipitation and western blot analysis. (d) RAW264.7 cells were treated with DMSO (vehicle, 12 h), L-NAME (2.5 mM, 1 h), or α -tocopherol (50 μ M, 12 h) and with LPS (1 μ g/ml) for the indicated times. N-Tyr SOCS1 in the whole-cell lysates of the RAW264.7 cells was detected by immunoprecipitation and western blot analysis. (e) RAW264.7 cells were transfected with a control empty plasmid or a Flag-SOCS1-expressing plasmid for 48 h, and Flag-SOCS1 expression was detected by western blot analysis. WT and Flag-SOCS1-transfected RAW264.7 cells were incubated with FITC-*E. coli* (10 μ g/ml) for the indicated times, and fluorescence was determined using a fluorescence plate reader. (f) RAW264.7 cells transfected with siN.C or siSOCS1 (20 nM) for 24 h were incubated with FITC-*E. coli* (10 μ g/ml) for the indicated times, and fluorescence was determined using a fluorescence plate reader. (g) RAW264.7 cells transfected with the control empty plasmid or Flag-SOCS1 plasmid were treated with SNP (100 μ M) for 3 h, followed by further incubation with FITC-*E. coli* (10 μ g/ml) for 30 min, and fluorescence was determined using a fluorescence plate reader. * p < 0.05, ** p < 0.01 compared with controls.

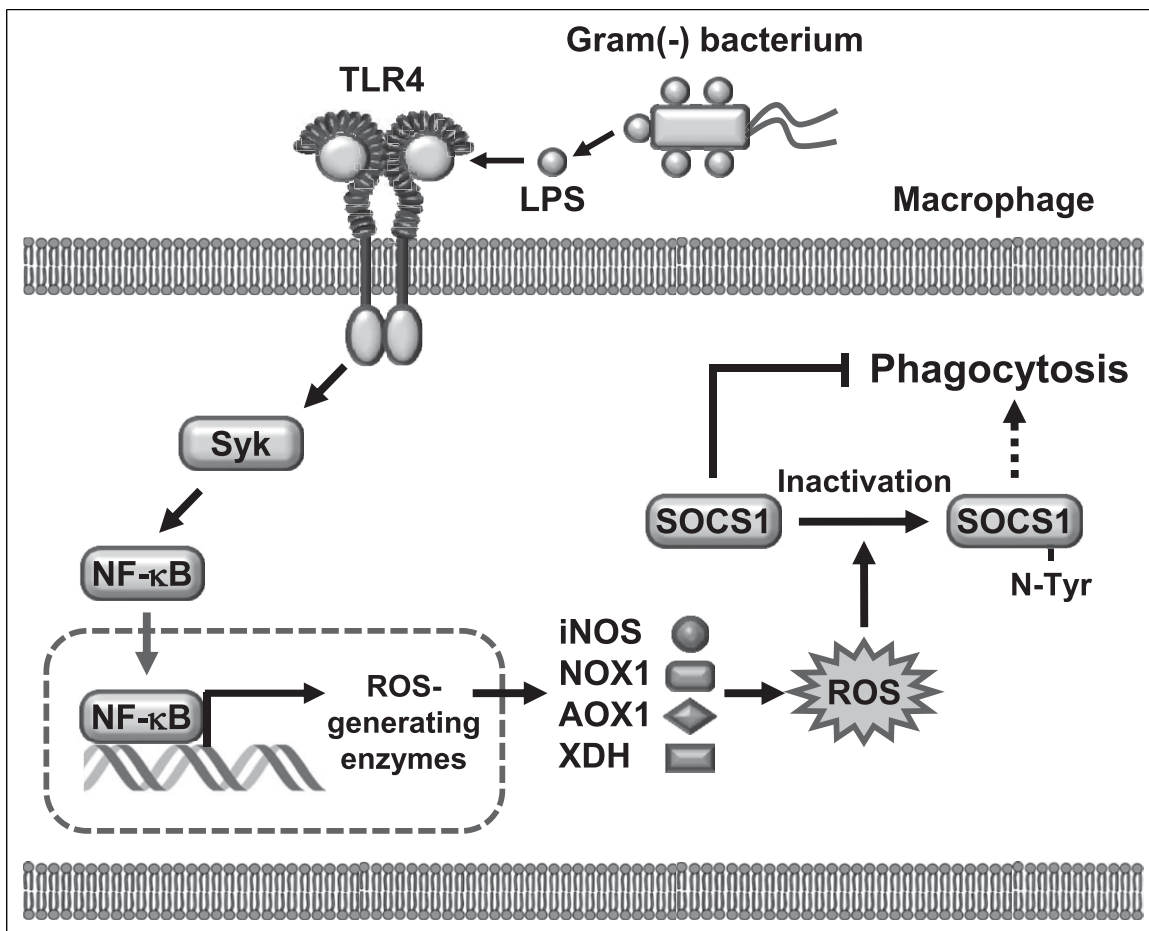


Figure 5. Schematic summary demonstrating the role of Syk in phagocytosis in macrophage-mediated inflammatory responses.

The role of Syk in the expression of ROS-generating enzymes in macrophages was examined to understand the molecular mechanism of Syk-induced ROS generation. Several ROS-generating enzymes have been identified. iNOS catalyzes L-arginine to produce NO,⁴⁵ and NOX1 produces ROS by oxidizing NADPH.⁴⁶ AOC3 catalyzes the oxidative deamination of primary amines, producing H₂O₂.⁴⁷ AOX1 produces ROS by oxidizing various aldehydes,⁴⁸ and XDH generates ROS by oxidizing ethanol.⁴⁹ The mRNA expression of those enzymes was increased in RAW264.7 cells following LPS treatment. Interestingly, the mRNA expression of iNOS, NOX1, AOX1, and XDH increased rapidly, within 10 min of treatment, whereas AOC3 mRNA expression increased gradually for up to 30 min after LPS stimulation (Figure 3(a)). This indicates that, although these are all ROS-generating enzymes, their modes of action in generating ROS during macrophage-mediated inflammatory responses differ. The mRNA expression of these enzymes induced by LPS was decreased markedly in Syk^{-/-} and Syk-deficient

RAW264.7 cells (Figures 3(b)–(d)), suggesting that Syk induces ROS generation by upregulating the expression of ROS-generating enzymes in macrophages during the inflammatory response.

A large number of studies have demonstrated that the function of many intracellular signaling molecules is modulated by protein modifications, such as phosphorylation and proteolytic processing, during inflammatory responses.^{3,5–7,12,50–53} Interestingly, this study found some proteins that are tyrosine-nitrated by LPS and identified the N-Tyr of SOCS1 during the LPS-stimulated inflammatory response (Figures 4(a) and (b)). Because Syk induced ROS generation under LPS-stimulated inflammatory conditions (Figure 2), the functional relationships between ROS and the N-Tyr of SOCS1 were investigated, and it was found that LPS-induced ROS generation induced the N-Tyr of SOCS1 in RAW264.7 cells (Figure 4(d)), indicating that Syk-induced ROS generation modulates the function of SOCS1 via N-Tyr. The phagocytic activity increased by Syk-induced ROS generation was inhibited by ROS scavengers (Figure 2), and the N-Tyr of SOCS1 induced by

LPS stimulation was inhibited dramatically by ROS scavengers (Figure 4(d)). These results implicate SOCS1 as a negative regulator of phagocytosis and show that the N-Tyr of SOCS1 induced by ROS generation inactivates SOCS1, explaining the induction of phagocytosis in macrophages during the inflammatory response. Nitration studies of manganese-dependent superoxide dismutase (MnSOD) and cytochrome c show that such modifications can lead to loss-of-function or gain-of-function, respectively, through structural protein modification.^{54–57} In the results of this study, SOCS1 overexpression decreased phagocytic activity (Figure 4(e)), and SOCS1 inhibition by siSOCS1 increased phagocytic activity in LPS-stimulated RAW264.7 cells (Figure 4(f)). Also, ROS generation recovered the phagocytic activity that was decreased by SOCS1 (Figure 4(g)). These results suggest that ROS generation inhibits SOCS1 function via the N-Tyr of SOCS1, leading to induction of phagocytic activity in macrophages.

Although these results clearly show that the role of Syk in the phagocytic activity of macrophages occurs through regulation of ROS generation and SOCS1 modification, only a murine macrophage cell line, RAW264.7, was used in this study. These results need to be further confirmed in primary cells, such as bone marrow-derived macrophages and circulating peripheral monocytes, and also in human macrophages, such as THP-1, U937, and primary monocytes/macrophages isolated from patients. Also, an in vivo study using Syk KO mice will be critical in supporting the in vitro results of this study. Moreover, the identification of N-Tyr site(s) on SOCS1 during inflammatory responses and the detailed mechanisms by which SOCS1 regulates phagocytosis surely need to be further investigated.

Conclusion

This study demonstrated the role of Syk in phagocytosis and the underlying molecular mechanisms of macrophagic inflammatory responses. Upon LPS stimulation, Syk induces ROS generation by upregulating the expression of ROS-generating enzymes, which increases the phagocytic activity of macrophages. A mechanistic study revealed that Syk-induced ROS generation facilitated the phagocytic activity of macrophages by inactivating SOCS1, a negative regulator of phagocytosis, via the N-Tyr of SOCS1 during the inflammatory response (Figure 5). This study was designed to contribute to the understanding of the role of Syk in phagocytosis and to elucidate its underlying molecular mechanism in macrophage-mediated inflammatory responses because selective Syk targeting is a promising strategy to prevent and treat inflammatory responses and diseases.

Author Contributions

Y.S.Y., H.G.K., J.H.K., and J.Y.C. conceived and designed the experiments. Y.S.Y., H.G.K., J.H.K., W.S.Y., E.K., J.G.P., and N.A. performed the experiments. Y.S.Y., H.G.K., J.H.K., N.P., and J.Y.C. analyzed the data. N.P. contributed reagents, materials, and analysis tools. Y.S.Y. and J.Y.C. wrote, reviewed, and edited the manuscript. All authors have read and approved the present manuscript.

Declaration of conflicting interests

The author(s) declared no potential conflicts of interest with respect to the research, authorship, and/or publication of this article.

Funding

The author(s) disclosed receipt of the following financial support for the research, authorship, and/or publication of this article: This research was funded by the National Research Foundation of Korea (NRF) (2017R1A6A1A03015642) and by Sungkyunwan University, Suwon, Korea (2021).

ORCID iD

Jae Youl Cho  <https://orcid.org/0000-0001-8141-9927>

References

1. Janeway CA Jr and Medzhitov R (2002) Innate immune recognition. *Annu Rev Immunol* 20: 197–216.
2. Vanbervliet-Defrance B, Delaunay T, Daunizeau T, et al. (2020) Cisplatin unleashes Toll-like receptor 3-mediated apoptosis through the downregulation of c-FLIP in malignant mesothelioma. *Cancer Lett* 472: 29–39.
3. Yi YS (2020) Functional crosstalk between non-canonical caspase-11 and canonical NLRP3 inflammasomes during infection-mediated inflammation. *Immunology* 159: 142–155.
4. Byeon SE, Yi YS, Oh J, et al. (2012) The role of Src kinase in macrophage-mediated inflammatory responses. *Mediat Inflamm* 2012: 512926.
5. Yu T, Yi YS, Yang Y, et al. (2012) The pivotal role of TBK1 in inflammatory responses mediated by macrophages. *Mediat Inflamm* 2012: 979105.
6. Yi YS, Son YJ, Ryou C, et al. (2014) Functional roles of Syk in macrophage-mediated inflammatory responses. *Mediat Inflamm* 2014: 270302.
7. Yang Y, Kim SC, Yu T, et al. (2014) Functional roles of p38 mitogen-activated protein kinase in macrophage-mediated inflammatory responses. *Mediat Inflamm* 2014: 352371.
8. Aderem A (2003) Phagocytosis and the inflammatory response. *J Infect Dis* 187(suppl 2): S340–S345.
9. Kourtzelis I, Hajishengallis G and Chavakis T (2020) Phagocytosis of apoptotic cells in resolution of inflammation. *Front Immunol* 11: 553.

10. Yi YS (2018) Regulatory Roles of the caspase-11 non-canonical inflammasome in inflammatory diseases. *Immune Network* 18: e41.
11. Hases L, Indukuri R, Birgersson M, et al. (2020) Intestinal estrogen receptor beta suppresses colon inflammation and tumorigenesis in both sexes. *Cancer Lett* 492: 54–62.
12. Yang WS, Yi YS, Kim D, et al. (2017) Nuclear factor kappa-B- and activator protein-1-mediated immunostimulatory activity of compound K in monocytes and macrophages. *Journal of Ginseng Research* 41: 298–306.
13. Yang J, Li Y, Sun Z and Zhan H (2021) Macrophages in pancreatic cancer: An immunometabolic perspective. *Cancer Lett* 498: 188–200.
14. Yi YS (2016) Folate receptor-targeted diagnostics and therapeutics for inflammatory diseases. *Immune Network* 16: 337–343.
15. Crusz SM and Balkwill FR (2015) Inflammation and cancer: advances and new agents. *Nat Rev Clin Oncol* 12: 584–596.
16. Yi YS (2019) Ameliorative effects of ginseng and ginsenosides on rheumatic diseases. *Journal of Ginseng Research* 43: 335–341.
17. Rowley RB, Bolen JB and Fargnoli J (1995) Molecular cloning of rodent p72Syk. Evidence of alternative mRNA splicing. *J Biol Chem* 270: 12659–12664.
18. Taniguchi T, Kobayashi T, Kondo J, et al. (1991) Molecular cloning of a porcine gene syk that encodes a 72-kDa protein-tyrosine kinase showing high susceptibility to proteolysis. *J Biol Chem* 266: 15790–15796.
19. Ziegenfuss JS, Biswas R, Avery MA, et al. (2008) Draper-dependent glial phagocytic activity is mediated by Src and Syk family kinase signalling. *Nature* 453: 935–939.
20. Steele RE, Stover NA and Sakaguchi M (1999) Appearance and disappearance of Syk family protein-tyrosine kinase genes during metazoan evolution. *Gene* 239: 91–97.
21. Xue L, Geahlen RL and Tao WA (2013) Identification of direct tyrosine kinase substrates based on protein kinase assay-linked phosphoproteomics. *Mol Cell Proteomics* 12: 2969–2980.
22. Mocsai A, Ruland J and Tybulewicz VL (2010) The SYK tyrosine kinase: a crucial player in diverse biological functions. *Nat Rev Immunol* 10: 387–402.
23. Lee YG, Chain BM and Cho JY (2009) Distinct role of spleen tyrosine kinase in the early phosphorylation of inhibitor of kappaB alpha via activation of the phosphoinositide-3-kinase and Akt pathways. *Int J Biochem Cell Biol* 41: 811–821.
24. Slomiany BL and Slomiany A (2019) Syk: a new target for attenuation of Helicobacter pylori-induced gastric mucosal inflammatory responses. *Inflammopharmacology* 27: 203–211.
25. Deng GM, Kyttaris VC and Tsokos GC (2016) Targeting Syk in Autoimmune Rheumatic Diseases. *Front Immunol* 7: 78.
26. Zarrin AA, Bao K, Lupardus P, et al. (2021) Kinase inhibition in autoimmunity and inflammation. *Nat Rev Drug Discov* 20: 39–63.
27. Kurniawan DW, Storm G, Prakash J, et al. (2020) Role of spleen tyrosine kinase in liver diseases. *World J Gastroenterol* 26: 1005–1019.
28. Shalem O, Sanjana NE, Hartenian E, et al. (2014) Genome-scale CRISPR-Cas9 knockout screening in human cells. *Science* 343: 84–87.
29. Yi YS, Jian J, Gonzalez-Gugel E, et al. (2018) Is Required for Canonical Lipopolysaccharide-induced TLR4 Signaling in Mice. *EBioMedicine* 29: 78–91.
30. Hirayama D, Iida T and Nakase H (2017) The phagocytic function of macrophage-enforcing innate immunity and tissue homeostasis. *Int J Mol Sci* 19: 92.
31. de Souza LF, Barreto F, da Silva EG, et al. (2007) Regulation of LPS stimulated ROS production in peritoneal macrophages from alloxan-induced diabetic rats: Involvement of high glucose and PPARgamma. *Life Sci* 81: 153–159.
32. Seow CJ, Chue SC and Wong WS (2002) Piceatannol, a Syk-selective tyrosine kinase inhibitor, attenuated antigen challenge of guinea pig airways in vitro. *Eur J Pharmacol* 443: 189–196.
33. Park JG, Son YJ, Yoo BC, et al. (2017) Syk plays a critical role in the expression and activation of IRAK1 in LPS-treated macrophages. *Mediat Inflamm* 2017: 1506248.
34. Thews O, Lambert C, Kelleher DK, et al. (2005) Possible protective effects of alpha-tocopherol on enhanced induction of reactive oxygen species by 2-methoxyestradiol in tumors. *Adv Exp Med Biol* 566: 349–355.
35. Wu CM, Cheng YL, Dai YH, et al. (2014) alpha-Tocopherol protects keratinocytes against ultraviolet A irradiation by suppressing glutathione depletion, lipid peroxidation and reactive oxygen species generation. *Biomedical Reports* 2: 419–423.
36. Cheng PW, Lee HC, Lu PJ, et al. (2016) Resveratrol inhibition of Rac1-derived reactive oxygen species by AMPK decreases blood pressure in a fructose-induced rat model of hypertension. *Sci Rep* 6: 25342.
37. Lin YT, Wu YC, Sun GC, et al. (2018) Effect of resveratrol on reactive oxygen species-induced cognitive impairment in rats with angiotensin II-induced early Alzheimer's disease (dagger). *J Clin Med* 7: 329.
38. Sekhar S, Sampath-Kumara KK, Niranjana SR, et al. (2015) Attenuation of reactive oxygen/nitrogen species with suppression of inducible nitric oxide synthase expression in RAW 264.7 macrophages by bark extract of Buchanania lanzan. *Phcog Mag* 11: 283–291.
39. Jerkic M, Sotov V and Letarte M (2012) Oxidative stress contributes to endothelial dysfunction in mouse models of hereditary hemorrhagic telangiectasia. *Oxid Med Cell Longev* 2012: 686972.

40. Lucas K and Maes M (2013) Role of the Toll Like receptor (TLR) radical cycle in chronic inflammation: possible treatments targeting the TLR4 pathway. *Mol Neurobiol* 48: 190–204.
41. Liu HT, Du YG, He JL, et al. (2010) Tetramethylpyrazine inhibits production of nitric oxide and inducible nitric oxide synthase in lipopolysaccharide-induced N9 microglial cells through blockade of MAPK and PI3K/Akt signaling pathways, and suppression of intracellular reactive oxygen species. *J Ethnopharmacol* 129: 335–343.
42. Gray MA, Choy CH, Dayam RM, et al. (2016) Phagocytosis Enhances Lysosomal and Bactericidal Properties by Activating the Transcription Factor TFEB. *Curr Biol* 26: 1955–1964.
43. Wong CO, Gregory S, Hu H, et al. (2017) Lysosomal Degradation Is Required for Sustained Phagocytosis of Bacteria by Macrophages. *Cell Host Microbe* 21: 719–730.
44. Covarrubias A, Byles V and Horng T (2013) ROS sets the stage for macrophage differentiation. *Cell Res* 23: 984–985.
45. Suschek CV, Schnorr O and Kolb-Bachofen V (2004) The role of iNOS in chronic inflammatory processes *in vivo*: is it damage-promoting, protective, or active at all? *Curr Mol Med* 4: 763–775.
46. Oh Y, Jung HR, Min S, et al. (2021) Targeting antioxidant enzymes enhances the therapeutic efficacy of the BCL-X_L inhibitor ABT-263 in KRAS-mutant colorectal cancers. *Cancer Lett* 497: 123–136.
47. Lyles GA (1996) Mammalian plasma and tissue-bound semicarbazide-sensitive amine oxidases: biochemical, pharmacological and toxicological aspects. *Int J Biochem Cell Biol* 28: 259–274.
48. Kundu TK, Hille R, Velayutham M, et al. (2007) Characterization of superoxide production from aldehyde oxidase: an important source of oxidants in biological tissues. *Arch Biochem Biophys* 460: 113–121.
49. Castro GD, Delgado de Layno AM, Costantini MH, et al. (2001) Cytosolic xanthine oxidoreductase mediated bioactivation of ethanol to acetaldehyde and free radicals in rat breast tissue. Its potential role in alcohol-promoted mammary cancer. *Toxicology* 160: 11–18.
50. Chen Y, Ho L and Tergaonkar V (2021) sORF-Encoded MicroPeptides: New players in inflammation, metabolism, and precision medicine. *Cancer Lett* 500: 263–270.
51. Yi YS (2020) Caspase-11 non-canonical inflammasome: Emerging activator and regulator of infection-mediated inflammatory responses. *Int J Mol Sci* 21: 2736.
52. Yun M and Yi YS (2020) Regulatory roles of ginseng on inflammatory caspases, executioners of inflammasome activation. *Journal of Ginseng Research* 44: 373–385.
53. Lu F, Zhao Y, Pang Y, et al. (2021) NLRP3 inflammasome upregulates PD-L1 expression and contributes to immune suppression in lymphoma. *Cancer Lett* 497: 178–189.
54. Yamakura F, Taka H, Fujimura T, et al. (1998) Inactivation of human manganese-superoxide dismutase by peroxynitrite is caused by exclusive nitration of tyrosine 34 to 3-nitrotyrosine. *J Biol Chem* 273: 14085–14089.
55. Abriata LA, Cassina A, Tortora V, et al. (2009) Nitration of solvent-exposed tyrosine 74 on cytochrome c triggers heme iron-methionine 80 bond disruption. Nuclear magnetic resonance and optical spectroscopy studies. *J Biol Chem* 284: 17–26.
56. You L and Cho JY (2021) The regulatory role of Korean ginseng in skin cells. *Journal of Ginseng Research* 45: 363–370.
57. Tian H, Kang Y, Song X, et al. (2020) PDL1-targeted vaccine exhibits potent antitumor activity by simultaneously blocking PD1/PDL1 pathway and activating PDL1-specific immune responses. *Cancer Lett* 476: 170–182.

Appendix

NF-κB	nuclear factor-κB
AP-1	activator protein-1
IRFs	interferon regulatory factors
Syk	spleen tyrosine kinase